Histologically normal human mammary epithelia with silenced *p16^{INK4a}* overexpress COX-2, promoting a premalignant program

Yongping G. Crawford,[1] Mona L. Gauthier,[1] Anita Joubel,[1] Kristin Mantei,[1,4] Krystyna Kozakiewicz,[1] Cynthia A. Afshari,[2,3] and Thea D. Tlsty[1,*]

[1]Department of Pathology and Comprehensive Cancer Center, University of California at San Francisco, San Francisco, California 94143
[2]National Institutes of Environmental Health Sciences, Research Triangle Park, North Carolina 27709
[3]Present address: Amgen Inc., 1 Amgen Center Drive, Mailstop 5-1-A, Thousand Oaks, California 91320.
[4]Present address: Department of Pathology, University of Washington, Seattle, Washington 98195.
*Correspondence: ttlsty@itsa.ucsf.edu

Summary

Breast tissue from healthy women contains variant mammary epithelial cells (vHMEC) exhibiting *p16^{INK4a}* promoter hypermethylation both in vivo and in vitro. When continuously cultured, vHMEC acquire telomeric dysfunction and produce the types of chromosomal abnormalities seen in premalignant lesions of cancer. We find that late passage vHMEC express elevated prostaglandin cyclo-oxygenase 2 (COX-2), which contributes to increased prostaglandin synthesis, angiogenic activity, and invasive ability. These data demonstrate the existence of human mammary epithelial cells with the potential to acquire multiple genomic alterations and phenotypes associated with malignant cells. Moreover, COX-2 overexpression coincides with focal areas of *p16^{INK4a}* hypermethylation in vivo, creating ideal candidates as precursors to breast cancer. These putative precursors can be selectively eliminated upon exposure to COX-2 inhibitors in vitro.

Introduction

Breast tissue from healthy women, when examined in vitro, contains a subpopulation of variant mammary epithelial cells (vHMEC, postselection, M0, or postsenescent HMEC) that have silenced *p16^{INK4a}* through hypermethylation of promoter sequences (Brenner et al., 1998; Foster et al., 1998; Huschtscha et al., 1998). These cells exhibit several properties that distinguish them from the majority of mammary epithelial cells that proliferate from a tissue explant (HMEC or preselection HMEC), including the silencing of *p16^{INK4a}* gene expression through promoter hypermethylation and the stabilization of p53 (Romanov et al., 2001). In culture, vHMEC proliferate an additional 30 to 50 generations beyond the time that the HMEC population activates a proliferative arrest before reaching a second population growth plateau, termed agonescence (Romanov et al., 2001). Remarkably, nearly 100% of vHMEC approaching agonescence exhibit telomeric dysfunction and acquire chromosomal defects, including aneuploidy, telomeric associations, and various other classes of structural abnormalities similar to those seen in the earliest lesions of breast cancer (Holst et al., 2003; Romanov et al., 2001; Tlsty et al., 2001). In a recent study, we found that a subpopulation of histologically normal human mammary tissues in vivo also contains cells with hypermethylated *p16^{INK4a}* promoter sequences. These cells were found in discrete foci in a substantial fraction of women with no indication or predisposition to breast cancer (Holst et al., 2003). We hypothesize that this subpopulation of vHMEC, which exists in vivo, has potential for progression to premalignant and ultimately malignant lesions of the breast. Therefore, characterization of these cells in vitro may provide molecular markers for identifying premalignant lesions of breast cancer in vivo as well as critical targets for therapeutic or preventive intervention.

In this study, we find that cyclo-oxygenase 2 (*COX-2*), a gene that is often overexpressed in many human cancers and contributes to colon cancer initiation and progression in murine models (Oshima et al., 1996), is upregulated in *p16^{INK4a}* hypermethylated mammary epithelia in vitro. This upregulation of COX-2 contributes to increased prostaglandin synthesis, increased endothelial cell invasion, and invasive ability in vHMEC and thus provides growth advantages to already genomically unstable cells. Ominously, we found that cells with *p16^{INK4a}* pro-

SIGNIFICANCE

Our studies provide molecular markers for identifying perhaps the earliest lesions of human breast cancer (i.e., premalignant mammary epithelial cells) and a molecular mechanism for their generation. Furthermore, our data indicate that these vHMEC with malignant phenotypes can be selectively eliminated, thus preventing their further progression. Finally, our study suggests that nonsteroidal antiinflammatory drugs (NSAIDs) can directly target epithelial cells for cancer prevention in addition to their effect in targeting stromal and inflammatory cells. These data point to a possible molecular mechanism through which NSAIDs reduce breast cancer risk.

moter hypermethylation and coincident intense COX-2 expression exist in histologically normal human tissues in vivo, creating ideal candidates for breast cancer precursors.

Results

Human mammary epithelial cells in agonescence express high levels of COX-2

To identify novel properties that distinguish vHMEC from HMEC, we compared the gene expression profiles of both cell populations as they progressed through increasing population doublings using microarrays. Primary explants from reduction mammoplasties from women ranging in age from 16 to 57 years were cultured as described previously to generate the growth curves for HMEC and vHMEC (Figure 1A). For this study, RNAs from cells at different passages in culture were compared to identify markers that change as the cells approach agonescence (Figure 1A). Among the genes that were upregulated in vHMEC at later passage or agonescence was *COX-2* (an ~6-fold induction between late and early vHMEC, Figure 1A, inset). This gene was of immediate interest, since several lines of evidence implicate COX-2 protein as an important modulator of tumor progression (Howe et al., 2001). We verified that the upregulation of COX-2 mRNA was indeed accompanied by an increase in protein expression via Western blot analysis (Figure 1B) and immunocytochemistry (Figure 1C). In these analyses, COX-2 expression was undetectable in the early HMEC population but increased significantly as vHMEC populations approached and entered agonescence (Figures 1B and 1C). Similar COX-2 upregulation in vHMEC was observed in samples derived from three additional individuals (Figure 1C and microarray data not shown). In a fifth case, low levels of COX-2 expression were observed in HMEC (RM9), and vHMEC from the same mammoplasty demonstrated similar COX-2 expression to that of the other vHMEC populations.

We further investigated the timing, heterogeneity, and level of COX-2 overexpression in individual vHMEC cells. Immunocytochemical analysis demonstrated that, while COX-2 was expressed at a high level in the majority of vHMEC at late passage, the protein was expressed at a similarly high level but in far fewer cells in vHMEC populations at early passage. Thus, the majority of the increase in COX-2 expression was the result of the induction of an increased number of cells exhibiting high expression (Figure 1C, right column) rather than a general increase in all cells. These data indicate that the loss of $p16^{INK4a}$ protein per se is not responsible for the induction of COX-2, since all early vHMEC cells in the population exhibit $p16^{INK4a}$ promoter hypermethylation, but only a few cells overexpress COX-2. Furthermore, expression of exogenous p16 protein in vHMEC overexpressing COX-2 does not suppress COX-2 overexpression (data not shown). Taken together, these data suggest that the lack of p16 activity may be permissive for a subsequent event, which then leads to the induction of COX-2 overexpression. Once this subsequent event occurs, the consequences cannot be suppressed by p16 expression.

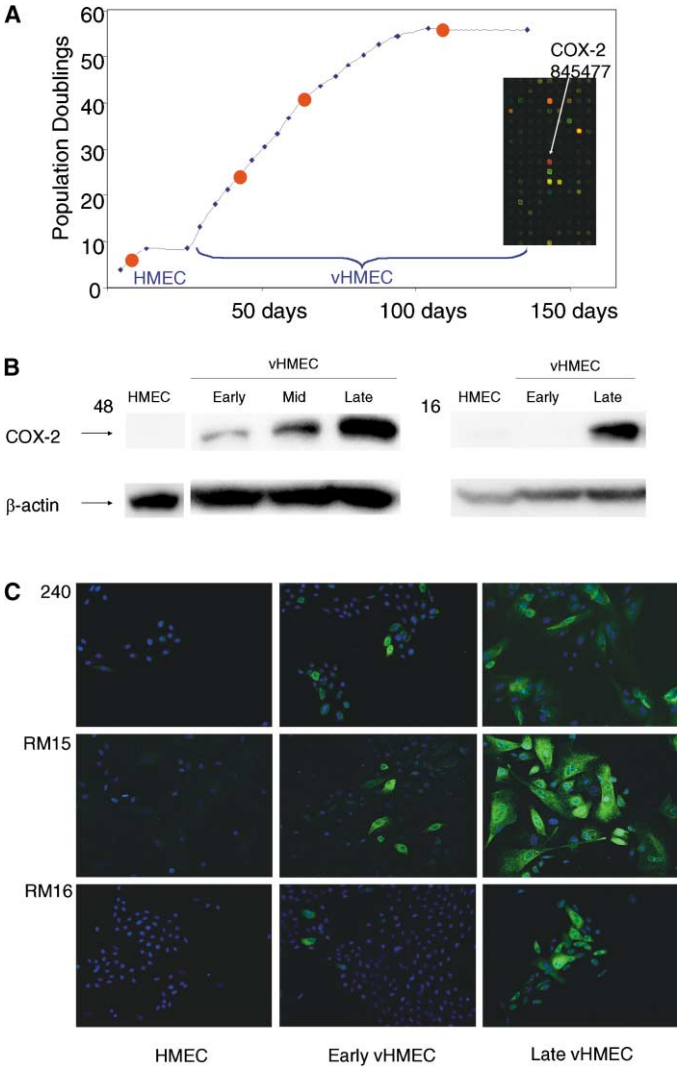

Figure 1. COX-2 expression is elevated in vHMEC in vitro

A: Representative HMEC/vHMEC 48 growth curve. Filled red circles indicate population doublings (PD) at which mRNA was isolated for microarray experiment. Inset: An example of microarray data showing the upregulation of COX-2 (arrow and red color).

B: Expression of human COX-2 protein quantity assessed by Western blot analysis. The following lysates from HMEC/vHMEC 48 were loaded: HMEC (PD 3), early passage vHMEC (PD 21), mid passage vHMEC (PD 34), and late passage vHMEC (PD 44). The following lysates from HMEC/vHMEC RM16 were loaded: HMEC (PD 4), early passage vHMEC (PD 18), and late passage vHMEC (PD 38).

C: Immunocytochemistry for COX-2 expression in HMEC, early, and late passage vHMEC 240 (PD 3, PD 25, and PD 46), RM15 (PD 3, PD 19, and PD 48), and RM16 (PD 3, PD 13, and PD 44), respectively.

High levels of COX-2 expression can be induced by DNA damage associated with telomeric dysfunction

An event that occurs subsequent to the loss of p16 protein activity and coincides with the increase in COX-2 overexpression is the increase in the number of cells exhibiting telomeric dysfunction (Figure 2A). Numerous studies have described how telomeric dysfunction can activate DNA damage response pathways (de Lange, 2002; Nautiyal et al., 2002). Therefore, we investigated the possibility that DNA damage signals such as those generated by telomeric dysfunction could induce COX-2. To experimentally induce a DNA damage response that mimics telomeric dysfunction, we exposed early passage vHMEC (with negligible COX-2 expression) to adriamycin, which was pre-

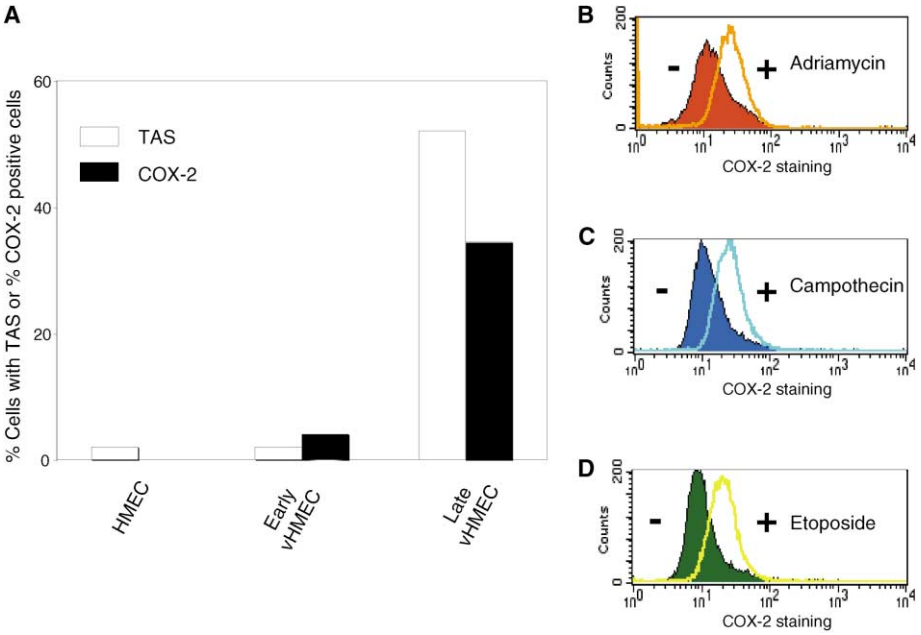

Figure 2. DNA damage induces COX-2 expression

A: Percent COX-2-positive vHMEC (48) increases as percent vHMEC exhibiting telomere association (TAS) increases. Percent COX-2-positive cells was determined using flow cytometry. TAS was scored as dicentric telomeres after G-banding karyotyping.

B–D: Flow analysis indicates that DNA-damaging agents adriamycin (1 μM), campothecin (2.5 μM), and etoposide (2.5 μM) induce COX-2 expression. Early vHMEC (RM16, PD 13, or PD 18) were incubated with adriamycin for 2 hr and with campothecin or etoposide for 6 hr and analyzed 24 hr later.

viously reported to cause telomeric dysfunction and result in telomere-related chromosomal abnormalities in breast tumor cells (Elmore et al., 2002). We found that early passage vHMEC exhibited a strong induction of COX-2 expression upon exposure to 1 μM adriamycin (Figure 2B). Additionally, we exposed early passage vHMEC to inhibitors for topoisomerases I and II (campothecin and etoposide, respectively), two agents that also generate DNA breaks similar to those produced by telomeric dysfunction (i.e., dicentric chromosomal breakage). Under both of these conditions, COX-2 was induced in a dose-dependent manner (Figures 2C and 2D and data not shown). A recent study demonstrated that DNA damage, induced by mitomycin C, also upregulates COX-2 (Han et al., 2002). Taken together, our data support the interpretation that DNA damage similar to that produced by telomeric dysfunction, an event that occurs in vHMEC subsequent to $p16^{INK4a}$ promoter hypermethylation, can contribute to the induction of COX-2 overexpression.

High levels of COX-2 expression in agonescent vHMEC confers malignant phenotypes

While the downstream effects of overexpressing COX-2 in tumor cells are well established, the phenotypes that accompany COX-2 overexpression in vHMEC are unknown. Comparison of vHMEC expressing a high level of COX-2 to those with a negligible level revealed significant differences in the expression of phenotypes hypothesized to be critical to malignancy (e.g., control of prostaglandin synthesis, angiogenesis, invasion, and apoptosis). vHMEC expressing a high level of COX-2 demonstrated a dramatic increase in the induction of prostaglandin E_2 (PGE_2), a direct product of COX-2 activity, as well as three other downstream products of COX-2 (6-keto $PGF_{1\alpha}$, $PGF_{2\alpha}$, and thromboxane B_2 [TXB_2]) when compared to cells expressing a negligible level of COX-2 (Figures 3A and 3B and data not shown) (RM16 and 48). Furthermore, vHMEC expressing a high level of COX-2 stimulated a significant increase in the invasion of human umbilical vein endothelial cells (HUVEC) across a collagen layer when compared to HMEC expressing a negligible level of COX-2 in an assay for inducing angiogenic ability (Figure 3C, black bars) in three vHMEC populations tested (RM15, RM16, and 48). Finally, vHMEC expressing a high level of COX-2 induced increased invasion of mammary epithelial cells across a Boyden chamber barrier when compared to HMEC expressing a negligible level of COX-2 (Figure 3D, black bars) in three vHMEC populations tested (RM15, RM16, and 48). Hence, both vHMEC and tumor cells, each overexpressing COX-2, exhibit similar phenotypes that contribute to malignant potential. Interestingly, conditioned media from the COX-2-overexpressing vHMEC did not demonstrate an ability to induce either HUVEC or mammary epithelial cell invasion across a collagen layer (Figures 3C and 3D, white bars). These data suggest that the downstream signal(s) of COX-2 that mediates both angiogenic and invasive activity is transient or short lived. Thus, constant COX-2 activity is required for the invasive phenotype induced by vHMEC.

To determine if the specific expression of COX-2 is necessary and/or sufficient for the exhibition of these malignant phenotypes, we manipulated COX-2 levels and documented the causal relationship between the two events. To remove elevated COX-2 expression from late passage vHMEC, we used both a chemical inhibitor and a COX-2 antisense construct. We exposed the late passage vHMEC to a specific COX-2 inhibitor, NS-398, for 24 hr and measured HUVEC invasion 12 hr later. We found that the originally observed HUVEC invasion (Figure 3C) was substantially reduced upon exposure to NS-398 (Figure 4A). We next introduced a COX-2 antisense construct under the control of tetracycline promoter into late vHMEC overexpressing COX-2 (RM16, PD 38; 48, PD 48). Four days after the addition of doxycycline, COX-2 protein levels were reduced in vHMEC containing a COX-2 antisense construct (Figure 4E, top panel). Furthermore, this reduction in COX-2 protein level was accompanied by a reduced level of excreted PGE_2 (Figure 4B). When these cells (RM16 and 48) were assayed for their ability to stimulate HUVEC invasion or movement of vHMEC across transwell

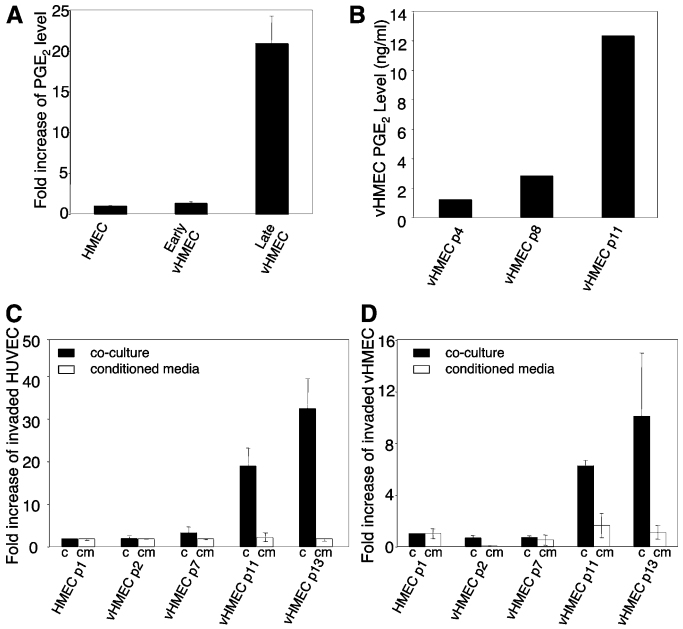

Figure 3. Late passage COX-2-overexpressing vHMEC exhibit increased PGE_2 production, angiogenic potential, and invasive ability

A: Fold induction in PGE_2 levels. PGE_2 levels were determined using ELISA assay (Cayman Chemical) and normalized to the number of cells (RM16) harvested. The level of PGE_2 for HMEC was set to be 1. Fold of PGE_2 induction for vHMEC was determined as the ratio of PGE_2 levels for vHMEC versus HMEC (mean ± SEM). RM16 HMEC and early and late vHMEC were at PD 5, PD 20, and PD 43, respectively.

B: PGE_2 concentration in media (determined using mass spectrometry at Vanderbilt University) increases as vHMEC (RM16 p4 or PD 20, p8 or PD 34, and p11 or PD 43) approach agonesence.

C: Late passage vHMEC (RM16) but not conditioned media from late passage vHMEC exhibit increased ability to summon HUVEC. "c" (black bar), experiment was done with HMEC or vHMEC. "cm" (white bar), conditioned media was used for the experiment.

D: Late passage vHMEC (RM16) but not conditioned media from late passage vHMEC exhibit increased ability to induce mammary epithelial cell invasion across a collagen layer. RM16 HMEC/vHMEC p1, p2, p7, p11, and p13 were at PD 2, PD 13, PD 30, PD 44, and PD 49, respectively.

All experiments in **C**–**D** were done in triplicate, and all data were normalized to the number of cells harvested. Data obtained for HMEC or conditioned media from HMEC within each experiment were set to be 1, and fold induction for vHMEC were determined as the ratio of vHMEC versus HMEC (mean ± SEM).

barrier, both phenotypes were substantially attenuated, dropping to the same levels observed after exposure to NS-398 (Figures 4C and 4D). Expression of an antisense RNA may trigger an interferon response as a consequence of dsRNA formation and an altered pattern of protein expression. To exclude the possibility that the activation of an interferon response caused the reduction in the phenotypes observed above, we induced an interferon response in our vHMEC cells (RM15, PD 25; RM 16, PD 30) by exposing them to human interferon β. We found that the addition of interferon β (5–100 unit/ml) for 2–6 days was sufficient to upregulate the expression of a cell surface protein, HLA-1, as previously reported (Satoh et al., 1995) (see Supplementary Figure S1 at http://www.cancercell.org/cgi/content/full/5/3/263/DC1). However, despite the activation of interferon response in these vHMECs, neither HUVEC invasion nor movement of vHMEC across transwell barrier was reduced (Supplementary Figure S2). Furthermore, the HLA-1 protein level was similar in cells expressing either a COX-2 antisense or the vector control (Supplementary Figure S3), and the growth kinetics (or population doublings) (Supplementary Figure S4) for vHMEC containing either a COX-2 antisense or a control construct remain the same after the induction of COX-2 antisense expression for a period of time, including the 4 days during which all the relevant experiments were done. Together, our data indicate that COX-2 plays a causal role in the induction of these phenotypes observed in late vHMEC.

To investigate the sufficiency of COX-2 in promoting the phenotypes observed, we introduced exogenous COX-2 into early vHMEC (RM15, PD 7; RM16, PD 10; and 48, PD 10) that exhibited a low level of endogenous COX-2 expression (Figure 4E, bottom panel). This increase in COX-2 protein level was accompanied by an increased level of excreted PGE_2 (Figure 4F), and we found an increase in HUVEC and vHMEC invasion phenotypes (Figures 4G and 4H) in all three vHMEC populations tested (RM15, RM16, and 48; only data for RM15 is shown). Interestingly, early vHMEC expressing exogenous COX-2 often demonstrated only a modest increase in the HUVEC and vHMEC invasion phenotypes when compared to late passage vHMEC overexpressing endogenous COX-2 (Figure 3C), despite the fact that their COX protein levels were similar (data not shown). These data suggest that early vHMEC but not late vHMEC may still maintain the ability to modulate COX-2-mediated phenotypes. Nevertheless, our data suggest that COX-2 overexpression alone is able to increase the HUVEC and vHMEC invasion phenotype. Together, our data demonstrate that COX-2 overexpression in late vHMEC is causal for the phenotypes that promote malignant potential.

Foci of histologically normal human mammary epithelia with *p16^{INK4a}* promoter methylation overexpress COX-2 in vivo

Our previous work identified focal aggregates of mammary epithelial cells that contained methylated *p16^{INK4a}* promoter sequences in a subgroup of reduction mammoplasties obtained from healthy women (Holst et al., 2003). As reported here, in vitro cultured vHMEC with methylated *p16^{INK4a}* promoter sequences have the ability not only to accumulate chromosomal abnormalities but also to induce malignant phenotypes by upregulating COX-2. These cells would be ideal candidates for precursors to premalignant lesions of breast cancer, an observation that provoked our search for these cells in vivo. As reported earlier, cells within histological sections containing the methylated *p16^{INK4a}* promoter sequences retained normal tissue architecture, as confirmed by hemotoxylin and eosin (H&E) staining of adjacent serial sections (Holst et al., 2003). Strikingly, COX-2 staining of the adjacent serial sections demonstrated that only samples with foci containing ductal or lobular epithelial cells with *p16^{INK4a}* promoter hypermethylation (yellow areas, Figure 5) exhibited intense COX-2 staining (red demarcations, Figure 5, samples 9698 and 9624). This colocalization of COX-2 protein staining and *p16^{INK4a}* promoter hypermethylation within the same cells is presented in a recently described mapping technique (Figure 5 and Holst et al., 2003), and examples of COX-2 staining are shown. In some places, the areas of intense COX-2 staining are seen beyond the individual ducts and lobules that contain luminal mammary epithelial cells with hypermethylation of *p16^{INK4a}* promoter sequences in the surrounding epithelial struc-

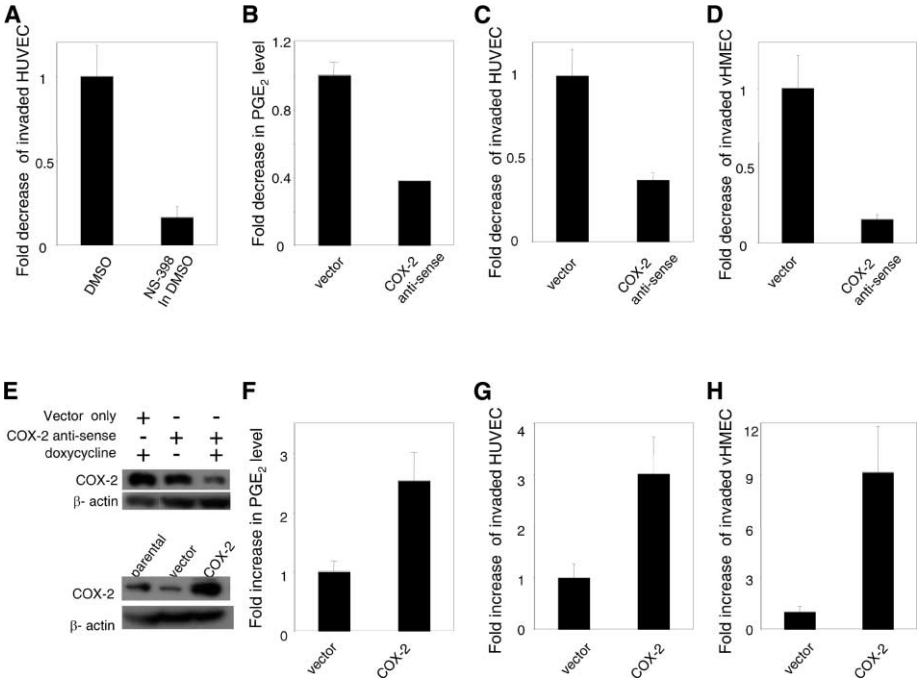

Figure 4. COX-2 contributes to the phenotypes observed in late vHMEC

A: COX-2 specific inhibitor NS-398 (25 μM) reduces the angiogenic activity in late vHMEC (RM16, PD 44). The experiment was carried out as above except that DMSO or NS-398 in DMSO was added to the media 24 hr before the assay. Data obtained for DMSO control was set to be 1, and fold change for vHMEC in NS-398 was determined as the ratio of vHMEC/NS-398 versus vHMEC/DMSO. Note: addition of NS-398 (25 μM) did not kill vHMEC within the 36 hr period exposure time.

B–D: Expression of COX-2 antisense RNA reduces PGE_2 level and reduced HUVEC and vHMEC invasion phenotypes, respectively, in late vHMEC (RM16, PD 44).

E: The top panel shows Western blot analysis for COX-2 protein level in late vHMEC with either vector control or COX-2 antisense with or without the addition of Doxycycline (RM16, PD 44). (Bottom panel) Western blot analysis for COX-2 protein level in early vHMEC (RM15, PD 7) with either vector or COX-2 overexpression construct.

F–H: Overexpression of COX-2 leads to increased PGE_2 level and increased HUVEC and vHMEC invasion phenotypes, respectively, in early vHMEC (RM15, PD 7). Similar results were observed with other RMs.

tures. This is possibly due to the diffusion of COX-2 products (e.g., prostaglandins) to the immediately adjacent areas, which upregulate COX-2 expression (Tjandrawinata and Hughes-Fulford, 1997). Alternatively, this may be due to an underestimate of the number of ducts and lobules that contain cells with hypermethylated *p16*^{INK4a} promoter sequences. The mammary tissue that expresses high COX-2 levels may have hypermethylation of adjacent CpG islands that are beyond the region of the *p16*^{INK4a} promoter sequences we investigated via methylation-specific PCR. In one sample, 10811, COX-2 staining was less intense than that observed in the other two samples with *p16*^{INK4a} silencing (Figure 5, sample 10811). This may reflect a cell population that has not yet fully sustained the events subsequent to *p16*^{INK4a} promoter hypermethylation that allow for full COX-2 induction or, alternatively, a cell population that has processed the events so that they no longer induce COX-2. Low to undetectable expression of COX-2 was observed in the majority of the tissue from the seven samples that were devoid of *p16*^{INK4a} promoter hypermethylation. Expression of COX-2 was largely devoid in surrounding stromal areas independent of *p16*^{INK4a} promoter hypermethylation status in the epithelial cells. These data demonstrate that foci of vHMEC in vivo exhibit elevated COX-2 expression.

vHMEC with high levels of COX-2 expression apoptose when exposed to a COX-2 inhibitor both in two-dimensional culture and in three-dimensional mammospheres

These newly described attributes of vHMEC have important clinical implications. Since COX-2 is known to inhibit apoptosis, inhibition of COX-2 functions may reinstate the apoptotic response and curtail the expansion of cells overexpressing COX-2. To this end, we exposed HMEC and vHMEC to various concentrations of NS-398, a specific COX-2 inhibitor (Liu et al., 1998), for 5 days and assayed its effect on viability. As shown in Figures 6A–6C, vHMEC that expressed high levels of COX-2 protein exhibited a significant decline in viability and activation of apoptosis as demonstrated by TUNEL analysis (Figure 6B). Upon exposure of the cells to NS-398 for 5 days, the majority of late passage vHMEC died, while, under identical conditions, the majority of the (non-COX-2-overexpressing) HMEC remained viable (Figures 6A–6C). This analysis was performed on four isogenic sets of HMEC and vHMEC with similar results (RM15, RM16, 48, and 240).

It has often been observed that therapeutic agents that are effective in two-dimensional assays may be ineffective when the cells are grown in three-dimensional structures (Hoffman, 1993). To better assess the potential of COX-2 inhibitors in vivo, we suspended HMEC and vHMEC (RM16 and 240) in reconstituted basement membrane, where they formed three-dimensional structures (mammospheres), and exposed these mammospheres to NS-398. Our results demonstrate that even when in three-dimensional structures, the COX-2 inhibitor effectively killed the COX-2-overexpressing vHMEC while having a negligible effect on HMEC (Figure 6D).

Discussion

In vivo foci of histologically normal mammary epithelial cells have silenced a tumor suppressor and activated a tumor-promoting program

Excitingly, our studies identify an in vivo population of mammary epithelial cells in disease-free women that have the ability to silence the tumor suppressor gene *p16*^{INK4a} through promoter hypermethylation and overexpress the tumor-promoting gene *COX-2*. Our studies also identify an in vitro population of variant mammary epithelial cells from disease-free women that, by loss of certain cell cycle checkpoint controls, have the ability to

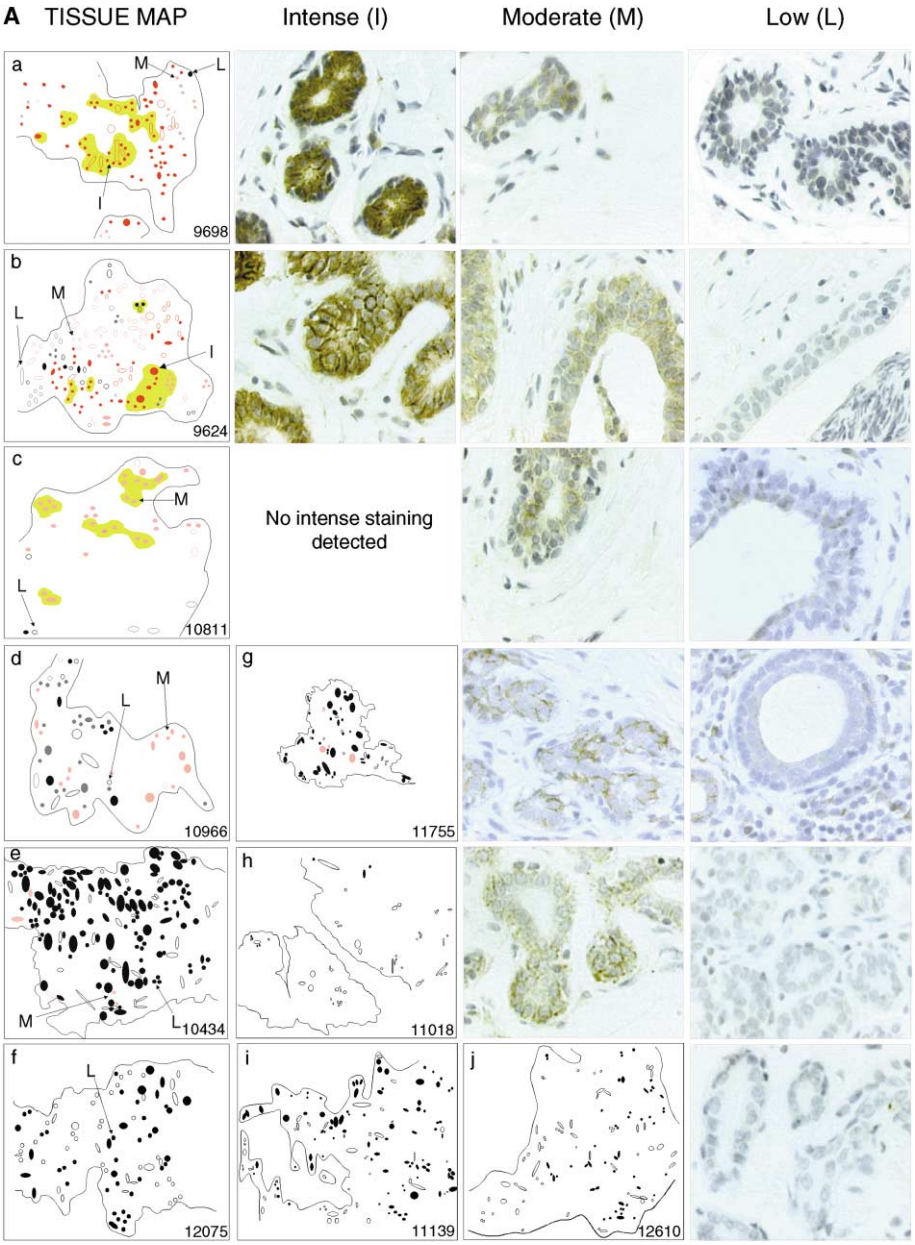

Figure 5. Intense COX-2 staining coincides with focal areas of *p16*^{INK4a} promoter hypermethylation in histologically normal tissue in vivo

Aa–Aj: We generated a gridded map of epithelial cell clusters by examining the H&E section at 40× magnification. All samples were determined to be histologically normal. Ductal clusters are illustrated as open ovals, lobular clusters as filled ovals, and foci of *p16*^{INK4a} promoter hypermethylation as yellow areas in **Aa**, **Ab**, and **Ac** (samples 9698, 9624, and 10811, respectively). In the adjacent serial sections, COX-2 expression level was qualitatively assessed by immunohistochemical staining and then scored as intense (red, >50% cells staining at highest intensity), moderate (pink, 1%–50% cells staining with heterogeneous low to moderate intensity), or low (black, 0%–<5% cells staining with low intensity). The examples of moderate COX-2 staining displayed in rows four and five are examples of the most intense staining observed in samples **Ad** and **Ae**. The few epithelial cell clusters that could not be assessed due to processing problems are gray. Regions of adipose tissue are not indicated for simplicity. Samples **Aa**, 9698; **Ab**, 9624; and **Ac**, 10811, each contain areas of *p16*^{INK4a} promoter hypermethylation as previously identified by in situ hybridization detection of methylation-specific PCR. Samples (**Ad**–**Aj**) 10966, 10434, 12075, 11755, 11018, 11139, and 12610, respectively, were previously determined to be devoid of foci with *p16*^{INK4a} promoter hypermethylation. The arrows indicate representative areas of intense (I), moderate (M), or low (L) staining for selected samples within that row. Note that, in the seven samples that were devoid of *p16*^{INK4a} promoter hypermethylation, we did not observe any areas of intense COX-2 staining. Differential fixation, processing, and sectioning of clinical specimens can contribute to heterogeneity of staining and limits quantitative analysis.

accumulate chromosomal abnormalities and express phenotypes that are critical to malignant progression. Without inactivation of pathways that prevent proliferation past a barrier, vHMEC could not proliferate to the point of telomeric crisis and undergo the sustained subsequent induction of COX-2. Thus, the initial checkpoint control defect, due in part to the epigenetic modulation of *p16*^{INK4a}, plays a crucial role in funneling cells into malignant pathways. The striking colocalization of COX-2 expression and *p16*^{INK4a} promoter hypermethylation within the same cells both in vivo and in vitro emphasizes the relevance of our in vitro studies in dissecting the early pathways leading to carcinogenesis.

Importantly, these studies also identify therapeutic targets that would allow for the elimination of these variant cells if they prove relevant to human disease. If variant cells were involved in disease progression, one would expect to find them in at least a fraction of premalignant lesions. Our recent finding of COX-2 overexpression in the majority of ductal carcinoma in situ (DCIS) lesions lends credence to this hypothesis (Shim et al., 2003). Even more intriguing was the finding that the histologically normal epithelial cells surrounding DCIS lesions, which were either positive or negative for COX-2 overexpression, also demonstrated increased expression of COX-2. These observations suggest that cells with overexpression of COX-2 may provide a fertile field for the emergence of premalignant lesions and, as discussed below, could be excellent targets for preventive therapy.

Several of the "hallmarks of cancer" are cocoordinately controlled by COX-2 expression

The colocalization of intense COX-2 staining in cells with hypermethylated *p16*^{INK4a} sequences has important implications for

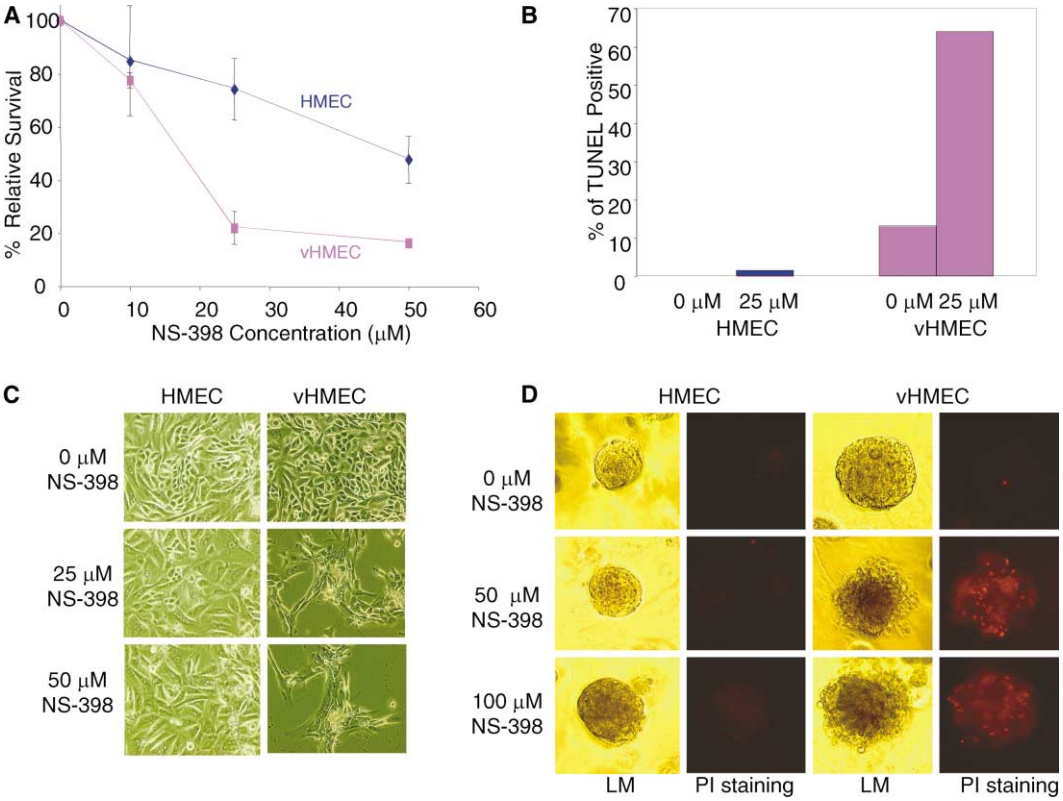

Figure 6. COX-2 inhibitor reduces cell survival of COX-2-expressing vHMEC

A: Percent survival of HMEC and vHMEC (RM16, PD 4 and PD 34) in the presence of various concentration of NS-398 after 5 days of incubation (mean ± SEM).

B: TUNEL experiment demonstrating the percentage of apoptotic cells after exposure to 25 μM NS-398 (RM16, PD 4 and PD 37).

C: Phase image of RM16 HMEC/vHMEC (PD 4 and PD 34) after incubation with 0, 25, and 50 μM NS-398 for 5 days.

D: Light microscopy (LM) and propidium iodine (PI) staining of HMEC and vHMEC (sample 240, PD 4 and PD 44) mammospheres in 3D culture after incubation with 0, 50, and 100 μM NS-398 for 5 days. Light microscopy illustrates the disrupted architecture of vHMEC mammospheres after incubation with NS-398. PI staining (red color) indicates cell death within vHMEC mammospheres after incubation with NS-398.

the initiation and progression of malignancy in breast tissue. COX-2 expression has been shown to be accompanied by phenotypes that are critically relevant to cancer development (Howe et al., 2001), several of which have been designated as "hallmarks of cancer" (Hanahan and Weinberg, 2000). COX-2 catalyzes the production of prostaglandins (PG_s), including prostaglandin E_2 (PDE_2), which stimulates mammary epithelial cell proliferation in the presence of EGF (Bandyopadhyay et al., 1987), and estrogen synthesis by activating aromatase (Harris et al., 1999). COX-2-induced PDE_2 also mediates immunosuppression by inhibiting T- and B-lymphocytes and cytokine production (Howe et al., 2001; Huang et al., 1998). Furthermore, the overexpression of COX-2 in tumor cells regulates angiogenesis, invasion, and apoptosis by promoting production of proangiogenic, proinvasive, and antiapoptotic factors (Gately, 2000; Tsujii and DuBois, 1995). Therefore, COX-2 expression in human mammary cells may provide sustained growth signals to mammary epithelial cells, protection from immune surveillance, and expression of malignant phenotypes. Our data (Figures 3 and 6) suggest that vHMEC containing hypermethylated $p16^{INK4a}$ promoter sequences and COX-2 overexpression exhibit malignant phenotypes such as increased angiogenesis and invasion and decreased apoptosis. Thus, they possess several characteristics identified as the hallmarks of cancer (Hanahan and Weinberg, 2000) and may represent a bona fide premalignant population. One characteristic these cells do not exhibit is unlimited replicative potential. In these cells, the loss of p16 allows an extended proliferative potential but not immortalization. Thus, we hypothesize that the overexpression of COX-2 enhances their malignant potential, priming them for malignant transformation, but additional alterations may be required for full transformation.

DNA damage and genomic instability lead to the induction of COX-2 and the activation of stromal and epithelial phenotypes crucial in malignant progression

Genomic instability plays a pivotal role in initiating and promoting the expression of malignant phenotypes on several levels. In human mammary epithelial cells, the hypermethylation of $p16^{INK4a}$ promoter sequence abrogates selected cell cycle checkpoint controls (Meyer et al., 1999) and allows the HMEC to bypass an in vitro growth barrier whose origin is currently unknown (Brenner et al., 1998; Romanov et al., 2001) (Figure 7). This loss of p16 protein relieves cyclin D1/cyclin-dependent kinase 4/6-control during G1/S transition and allows the subsequent unrestrained phosphorylation of pRB by cdk4/6 (T.D.T,

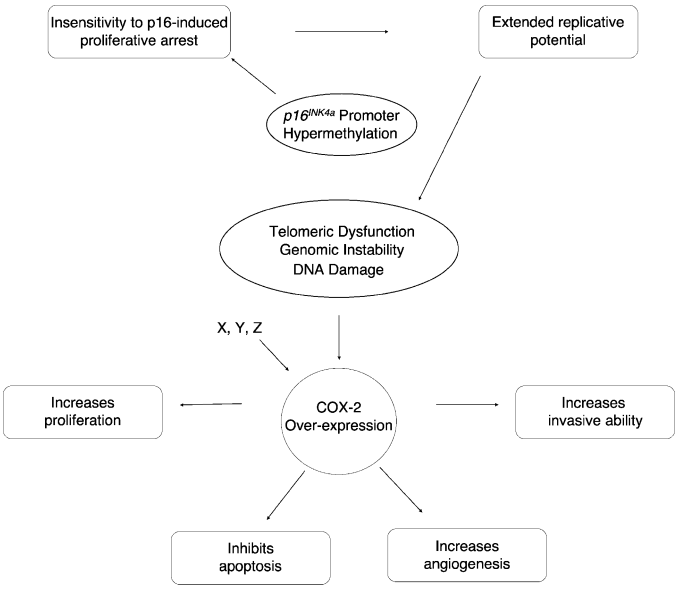

Figure 7. Genomic instability potentiates premalignant programs

p16^{INK4a} promoter sequence hypermethylation allows cells to proliferate until acquiring telomeric dysfunction. Genomic instability generated by chromosomal breakage associated with telomeric dysfunction is pivotal in activating multiple phenotypes associated with cancer through the upregulation of a single gene, COX-2. COX-2 can also be induced via other pathways indicated in the figure as X, Y, Z.

unpublished data). In the absence of these restraints and the presence of adequate nutrients and mitogenic factors, the vHMEC have an extended replicative potential (Brenner et al., 1998; Romanov et al., 2001). As vHMEC further proliferate, they continue to erode telomeric sequences until they experience telomeric dysfunction and initiate a cascade of genomic instability (Romanov et al., 2001). Telomere dysfunction not only provides genetic mutations required for cancer initiation (Maser and DePinho, 2002) but also instigates an apoptotic response (Karlseder et al., 1999). Studies in this report suggest that vHMEC with telomere dysfunction may also oppose these death signals by inducing COX-2, an antiapoptotic regulator, and thus allow the further proliferation of otherwise unviable cells. Concomitantly, these cells acquire malignant phenotypes that act within the epithelial cell as well as in the surrounding stroma (i.e., increased angiogenic response). The COX-2-induced inhibition of apoptosis and immune surveillance, along with the acquisition of invasive abilities, generates a population of epithelial cells that are poised for malignant progression. Furthermore, the COX-2-induced remodeling of the stroma, along with the induction of angiogenesis, supports this malignant program. Thus, we postulate that the two events of genomic instability, epigenetic modulation of *p16*^{INK4a} and chromosomal breaks generated by telomeric dysfunction, provide the initiating and promoting forces that drive the acquisition of a premalignant program (Figure 7). Subsequent induction of COX-2 (and other gene alterations) provide growth advantages to these otherwise compromised cells. While we do not suggest that all cancers arise in this manner, we do suggest that the critical events in this process (loss of cell cycle checkpoint control, telomere dysfunction, DNA damage, and sustained induction of COX-2) provide a mechanistic framework for malignant transformation.

NSAIDs target overexpression of COX-2 in mammary epithelia in addition to stroma acting both early and late in malignant progression

The first convincing evidence linking COX-2 to tumor initiation and progression came from studies in APC-deficient, COX-2 null mice (Oshima et al., 1996). The lack of COX-2 (either through genetic or pharmacological manipulation) reduces the incidence of intestinal adenomas and tumor size (Alshafie et al., 2000; Harris et al., 2000; Nakatsugi et al., 2000; Robertson et al., 1998). While the removal of COX-2 function suppresses tumor initiation and progression, the overexpression of COX-2 exacerbates the process in murine models. Oshima et al. provide genetic evidence that the induction of COX-2 is an early, rate-limiting step for adenoma formation (Oshima et al., 1996). Furthermore, tissue-specific overexpression of COX-2 from a mouse mammary tumor virus (MMTV) promoter was sufficient to cause mammary tumors in multiparous mice (Liu et al., 2001). These results in murine models strongly suggest that COX-2 is an important modulator of both tumor initiation and progression.

In humans, COX-2 also plays a dual role in carcinogenesis. The overexpression of COX-2 is often observed in multiple human tumors, including breast, colon, pancreas, and prostate (Soslow et al., 2000; Tucker et al., 1999). Additionally, and consistent with our view that COX-2 may play a role in early steps of carcinogenesis, epidemiological data suggest regular use of nonsteroidal antiinflammatory drugs (NSAIDs), including aspirin, which inhibits COX-2, reduces both sporadic and familial colon cancer incidence (Gupta and Dubois, 2001; Thun et al., 1991). Other studies point to a similar NSAID effect for breast and pancreatic cancer incidence (Friedman and Ury, 1980; Harris et al., 1996; Schreinemachers and Everson, 1994; Sharpe et al., 2000). A recent large prospective cohort study involving over 80,000 postmenopausal women indicated that there was a 21% and 28% reduction in the risk of breast cancer for women who took NSAIDs at least twice a week for at least 5–10 years when compared to women who reported no or minimal NSAIDs usage (Harris et al., 2003). These data, in conjunction with our observations of histologically normal human tissue in this report and studies from murine models, suggest that COX-2 functions both early and late in tumor progression and highlight COX-2 as a potential target for preventive therapy.

Conclusion

In summary, we demonstrate intense expression of COX-2 protein colocalized with *p16*^{INK4a} promoter hypermethylation in human mammary epithelial cells both in vitro and in vivo. COX-2 expression in these cells parallels the acquisition of telomeric dysfunction and can be induced by DNA damage. Further, COX-2 overexpression together with *p16*^{INK4a} promoter hypermethylation generates critical phenotypes that are believed to be instrumental in the progression to malignancy. Our data also indicate that NSAIDs can directly target epithelial cells for cancer prevention in addition to their effect in targeting stromal and inflammatory cells. Finally, the identification of differentially expressed genes in vHMEC not only allows for the identification of early lesions of breast cancer but also suggests targets for the selective removal of these putative precursor cells from the body.

Experimental procedures

Cells and cell culture

Isolation and culture of HMEC in modified MCDB 170 (MEGM, BioWhittaker) has been described (Hammond et al., 1984). We studied HMEC/vHMEC from reduction mammoplasty specimens from five individuals: HMEC/vHMEC 48, HMEC/vHMEC 240 (kindly provided by Martha Stampfer), HMEC/vHMEC RM9, RM15, and RM16 (cells derived in our laboratory). Population doublings (PD) were calculated using the equation PD = log(A/B)/log2, where A is the number of cells collected, and B is the number of cells plated.

Microarray experiment

Total RNA was isolated from HMEC (individual 48) using Qiagen Rneasy midi kit (Qiagen, Valencia, CA). Filled red circles in Figure 1A indicate points in the growth curve when mRNAs were isolated. The microarray experiments were performed at the National Institute of Environmental Health Sciences Microarray Center (Research Triangle Park, NC). Detailed protocols for microarray procedures are available at http://dir.niehs.nih.gov/microarray.

Immunohistochemistry

Five-micron sections were cut from routinely fixed paraffin-embedded tissue blocks and mounted on SuperFrost Plus microscope slides (Fisher Scientific, Pittsburgh, PA). Specimens were stepwise deparaffinized in xylene and rehydrated in descending alcohols. Endogenous peroxidase activity was blocked by incubation in 3% hydrogen peroxide in methanol for 10 min. Sections were microwaved for antigen retrieval for 10 min in a 10 mM citrate buffer (pH 6.0). Sections were rinsed in PBS and incubated for 30 min in blocking buffer (10% horse serum and 1% bovine serum albumin [BSA] in PBS), and immunostaining was performed using a COX-2 specific anti-human mouse monoclonal antibody (Cayman Chemical, No. 160112, Ann Arbor, MI) diluted 1:200 in 1% BSA in PBS overnight at 4°C. Control sections received human COX-2 control peptide (40 μg/ml; Cayman Chemical) along with the COX-2 primary antibody (incubated for 1 hr prior to application). Sections were rinsed in 0.05% Tween-20 in PBS followed by incubation in a biotinylated IgG anti-mouse secondary (Vector Laboratories, No. BA-2000, Burlingame, CA) made in horse diluted 1:200 in 1% BSA in PBS. Slides were rinsed in PBS and incubated in avidin-biotin horseradish peroxidase complex (Vector Laboratories, No. PK-6100, Vectastain Elite ABC kit) at a 1:100 dilution in 1% BSA in PBS for 30 min. Specimens were rinsed in 0.05% Tween-20 in PBS and incubated with 3,3′-diaminobenzadine (DAB) chromogenic substrate (Sigma Chemical, No. D-5905, St. Louis, MO) for 4 min. Sections were counterstained in hematoxylin, stepwise dehydrated through graded alcohols, and cleared in xylene before mounting using permount.

Western blot analysis

Thirty micrograms of protein from total cell extracts was fractionated in gradient (4%–20%) polyacrylamide gels (FMC) and transferred to Hybond-P (Amersham) membrane. Lysates were sequentially exposed to rabbit polyclonal anti-human COX-2 antibody (Oxford Research Biochemical and/or Cayman Chemical Co.) followed by horseradish peroxidase (HRP)-conjugated goat-anti-rabbit antibody (Gibco).

Flow analysis

Cells were fixed with 1% PFA and permeablized with 0.3% Triton X-100. Subsequent flow analysis was performed using FITC-conjugated anti-COX-2 antibody (Cayman Chemical, No. 160113).

Measurement of angiogenesis and invasion

Various HMEC and vHMEC were plated onto 24-well plates at a density that would reach 80% confluency 3 days later. HUVEC (from ATCC) or HMEC were plated onto inserted chambers at a density of 3×10^4/chamber. The number of cells moving across a collagen layer was determined by trypan blue staining and adjusted to the number of HMEC or vHMEC in each 24-well plate. Fold of induction in invaded HUVEC or HMEC was determined when compared to HMEC, which was then set to be 1. Each experiment was done in triplicate. For experiments involving cells with vector only, COX-2 antisense construct, or COX-2 overexpression construct, fold changes were determined when compared to vector control cells, which was set to be 1. Each experiment was done six times.

PGE_2 measurement

PGE_2 was determined using Prostaglandin E_2-Monoclonal Enzyme Immunoassay kit (Cayman Chemical). Each experiment was carried out in triplicate according to the manufacturer's protocol.

Expression of COX-2 sense and antisense constructs

COX-2 sense construct was packaged in Phoenix A cells for viral propagation. Viral supernatant was diluted 1:1 with MEGM media and then added to the early vHMEC twice consecutively. vHMEC infected with retroviruses were selected and maintained in 2 μg/ml puromycin. The tetracycline-on gene expression plasmid pUHD.2neo expressing the COX-2 antisense was transfected into late vHMECs using Lipofectamine 2000 (Invitrogene). Stable clones of vHMEC containing COX-2 antisense construct were selected and maintained in 70 μg/ml of Geneticin (GibcoBRL). To induce the expression of COX-2 antisense, 2 μg/ml doxycycline (Clontech) was added to the media prior to the experiments.

NS-398 inhibition

NS-398 (Cayman Chemical Company, Ann Arbor, MI) was dissolved in DMSO to generate 10 mM and 100 mM stock solutions. All final concentrations of NS-398 used for the experiments were diluted in the same amount of DMSO and made fresh for each usage. For two-dimensional culture, vHMEC were trypsinized and plated at a density of 2×10^4 cells per well in a 6-well plate for exposure of cells to 0, 10, and 25 μM and 5×10^4 per well for cells exposed to 50 μM NS-398. HMEC were treated similarly, except 3.5×10^4 cells per well were plated for exposure to 50 μM NS-398. NS-398 was applied to cells 1 day after initial seeding and every other day thereafter via a media change. Cells were harvested on the sixth day, and the numbers of live and total cells for each experiment were determined using the trypan blue exclusion assay. Percent survival was calculated as the number of live cells divided by the number of total cells in 0 μM NS-398 and adjusted according to the initial number of cells seeded. The relative percent survival for cells in 0 μM NS-398 was set to be 100%. The relative percent survival for cells in 10, 25, and 50 μM were calculated as the ratio between the percent of survival at various NS-398 concentrations and the percent survival at 0 μM NS-398. This experiment was done in triplicate for each of four sets of HMEC/vHMEC pairs. For 3D culture, HMEC/vHMEC were trypsinized and suspended in Matrigel (BD Bioscience, Bedford, MA) at a density of 5×10^4 cells/300 μl. Cells were allowed to form 3D structures for 10 days followed by exposure to 0, 50, and 100 μM NS-398. Five days after applying NS-398, cells were stained with propidium iodide (PI) without fixation and imaged using IP lab image software.

TUNEL assay

TUNEL experiments were performed according to the manufacturer's protocol from Clontech.

Acknowledgments

We thank J. Li, G. Evan, Z. Werb, and members of the Tlsty laboratory for helpful comments and criticism. We would like to gratefully acknowledge S. Grissom, L. Annab, and J. Collins at NIEHS for technical assistance in the microarray analysis; Dr. Robert Coffey and Dr. Jason Morrow at Vanderbilt University for assistance in determining levels of downstream products of COX-2 and kindly providing the COX-2 antisense construct; and Dr. Dan Dixon for providing COX-2 expression construct, from which we cloned human COX-2 into pLPCX and pLXSP vector. We also thank members of the UCSF Bay Area Breast SPORE Tissue Core facility for their advice with immunohistochemical staining. This work was supported by the Avon Foundation, The Cancer League, Inc., and grants from NIH and NIH/NASA awarded to T.D.T.

Received: March 27, 2003
Revised: December 17, 2003
Accepted: January 14, 2004
Published: March 22, 2004

References

Alshafie, G.A., Abou-Issa, H.M., Seibert, K., and Harris, R.E. (2000). Chemotherapeutic evaluation of Celecoxib, a cyclooxygenase-2 inhibitor, in a rat mammary tumor model. Oncol. Rep. *7*, 1377–1381.

Bandyopadhyay, G.K., Imagawa, W., Wallace, D., and Nandi, S. (1987). Linoleate metabolites enhance the in vitro proliferative response of mouse mammary epithelial cells to epidermal growth factor. J. Biol. Chem. *262*, 2750–2756.

Brenner, A.J., Stampfer, M.R., and Aldaz, C.M. (1998). Increased p16 expression with first senescence arrest in human mammary epithelial cells and extended growth capacity with p16 inactivation. Oncogene *17*, 199–205.

de Lange, T. (2002). Protection of mammalian telomeres. Oncogene *21*, 532–540.

Elmore, L.W., Rehder, C.W., Di, X., McChesney, P.A., Jackson-Cook, C.K., Gewirtz, D.A., and Holt, S.E. (2002). Adriamycin-induced senescence in breast tumor cells involves functional p53 and telomere dysfunction. J. Biol. Chem. *277*, 35509–35515.

Foster, S.A., Wong, D.J., Barrett, M.T., and Galloway, D.A. (1998). Inactivation of p16 in human mammary epithelial cells by CpG island methylation. Mol. Cell. Biol. *18*, 1793–1801.

Friedman, G.D., and Ury, H.K. (1980). Initial screening for carcinogenicity of commonly used drugs. J. Natl. Cancer Inst. *65*, 723–733.

Gately, S. (2000). The contributions of cyclooxygenase-2 to tumor angiogenesis. Cancer Metastasis Rev. *19*, 19–27.

Gupta, R.A., and Dubois, R.N. (2001). Colorectal cancer prevention and treatment by inhibition of cyclooxygenase-2. Nat. Rev. Cancer *1*, 11–21.

Hammond, S.L., Ham, R.G., and Stampfer, M.R. (1984). Serum-free growth of human mammary epithelial cells: rapid clonal growth in defined medium and extended serial passage with pituitary extract. Proc. Natl. Acad. Sci. USA *81*, 5435–5439.

Han, J.A., Kim, J.I., Ongusaha, P.P., Hwang, D.H., Ballou, L.R., Mahale, A., Aaronson, S.A., and Lee, S.W. (2002). P53-mediated induction of Cox-2 counteracts p53- or genotoxic stress-induced apoptosis. EMBO J. *21*, 5635–5644.

Hanahan, D., and Weinberg, R.A. (2000). The hallmarks of cancer. Cell *100*, 57–70.

Harris, R.E., Namboodiri, K.K., and Farrar, W.B. (1996). Nonsteroidal antiinflammatory drugs and breast cancer. Epidemiology *7*, 203–205.

Harris, R.E., Robertson, F.M., Abou-Issa, H.M., Farrar, W.B., and Brueggemeier, R. (1999). Genetic induction and upregulation of cyclooxygenase (COX) and aromatase (CYP19): an extension of the dietary fat hypothesis of breast cancer. Med. Hypotheses *52*, 291–292.

Harris, R.E., Alshafie, G.A., Abou-Issa, H., and Seibert, K. (2000). Chemoprevention of breast cancer in rats by celecoxib, a cyclooxygenase 2 inhibitor. Cancer Res. *60*, 2101–2103.

Harris, R.E., Chlebowski, R.T., Jackson, R.D., Frid, D.J., Ascenseo, J.L., Anderson, G., Loar, A., Rodabough, R.J., White, E., and McTiernan, A. (2003). Breast cancer and nonsteroidal anti-inflammatory drugs: prospective results from the Women's Health Initiative. Cancer Res. *63*, 6096–6101.

Hoffman, R.M. (1993). To do tissue culture in two or three dimensions? That is the question. Stem Cells *11*, 105–111.

Holst, R.H., Nuovo, G.J., Esteller, M., Chew, K., Baylin, S.B., Herman, J.G., and Tlsty, T.D. (2003). Methylation of p16INK4a promoters occurs in vivo in histologically normal human mammary epithelia. Cancer Res., in press.

Howe, L.R., Subbaramaiah, K., Brown, A.M., and Dannenberg, A.J. (2001). Cyclooxygenase-2: a target for the prevention and treatment of breast cancer. Endocr. Relat. Cancer *8*, 97–114.

Huang, M., Stolina, M., Sharma, S., Mao, J.T., Zhu, L., Miller, P.W., Wollman, J., Herschman, H., and Dubinett, S.M. (1998). Non-small cell lung cancer cyclooxygenase-2-dependent regulation of cytokine balance in lymphocytes and macrophages: up-regulation of interleukin 10 and down-regulation of interleukin 12 production. Cancer Res. *58*, 1208–1216.

Huschtscha, L.I., Noble, J.R., Neumann, A.A., Moy, E.L., Barry, P., Melki, J.R., Clark, S.J., and Reddel, R.R. (1998). Loss of p16INK4 expression by methylation is associated with lifespan extension of human mammary epithelial cells. Cancer Res. *58*, 3508–3512.

Karlseder, J., Broccoli, D., Dai, Y., Hardy, S., and de Lange, T. (1999). p53- and ATM-dependent apoptosis induced by telomeres lacking TRF2. Science *283*, 1321–1325.

Liu, X.H., Yao, S., Kirschenbaum, A., and Levine, A.C. (1998). NS398, a selective cyclooxygenase-2 inhibitor, induces apoptosis and down-regulates bcl-2 expression in LNCaP cells. Cancer Res. *58*, 4245–4249.

Liu, C.H., Chang, S.H., Narko, K., Trifan, O.C., Wu, M.T., Smith, E., Haudenschild, C., Lane, T.F., and Hla, T. (2001). Overexpression of cyclooxygenase-2 is sufficient to induce tumorigenesis in transgenic mice. J. Biol. Chem. *276*, 18563–18569.

Maser, R.S., and DePinho, R.A. (2002). Connecting chromosomes, crisis, and cancer. Science *297*, 565–569.

Meyer, K.M., Hess, S.M., Tlsty, T.D., and Leadon, S.A. (1999). Human mammary epithelial cells exhibit a differential p53-mediated response following exposure to ionizing radiation or UV light. Oncogene *18*, 5795–5805.

Nakatsugi, S., Ohta, T., Kawamori, T., Mutoh, M., Tanigawa, T., Watanabe, K., Sugie, S., Sugimura, T., and Wakabayashi, K. (2000). Chemoprevention by nimesulide, a selective cyclooxygenase-2 inhibitor, of 2-amino-1-methyl-6-phenylimidazo[4,5-b]pyridine (PhIP)-induced mammary gland carcinogenesis in rats. Jpn. J. Cancer Res. *91*, 886–892.

Nautiyal, S., DeRisi, J.L., and Blackburn, E.H. (2002). The genome-wide expression response to telomerase deletion in Saccharomyces cerevisiae. Proc. Natl. Acad. Sci. USA *99*, 9316–9321.

Oshima, M., Dinchuk, J.E., Kargman, S.L., Oshima, H., Hancock, B., Kwong, E., Trzaskos, J.M., Evans, J.F., and Taketo, M.M. (1996). Suppression of intestinal polyposis in Apc delta716 knockout mice by inhibition of cyclooxygenase 2 (COX-2). Cell *87*, 803–809.

Robertson, F.M., Parrett, M.L., Joarder, F.S., Ross, M., Abou-Issa, H.M., Alshafie, G., and Harris, R.E. (1998). Ibuprofen-induced inhibition of cyclooxygenase isoform gene expression and regression of rat mammary carcinomas. Cancer Lett. *122*, 165–175.

Romanov, S.R., Kozakiewicz, B.K., Holst, C.R., Stampfer, M.R., Haupt, L.M., and Tlsty, T.D. (2001). Normal human mammary epithelial cells spontaneously escape senescence and acquire genomic changes. Nature *409*, 633–637.

Satoh, J., Paty, D.W., and Kim, S.U. (1995). Differential effects of beta and gamma interferons on expression of major histocompatibility complex antigens and intercellular adhesion molecule-1 in cultured fetal human astrocytes. Neurology *45*, 367–373.

Schreinemachers, D.M., and Everson, R.B. (1994). Aspirin use and lung, colon, and breast cancer incidence in a prospective study. Epidemiology *5*, 138–146.

Sharpe, C.R., Collet, J.P., McNutt, M., Belzile, E., Boivin, J.F., and Hanley, J.A. (2000). Nested case-control study of the effects of non-steroidal anti-inflammatory drugs on breast cancer risk and stage. Br. J. Cancer *83*, 112–120.

Shim, V., Gauthier, M.L., Sudilovsky, D., Mantei, K., Chew, K.L., Moore, D.H., Cha, I., Tlsty, T.D., and Esserman, L.J. (2003). Cyclooxygenase-2 expression is related to nuclear grade in ductal carcinoma in situ and is increased in its normal adjacent epithelium. Cancer Res. *63*, 2347–2350.

Soslow, R.A., Dannenberg, A.J., Rush, D., Woerner, B.M., Khan, K.N., Masferrer, J., and Koki, A.T. (2000). COX-2 is expressed in human pulmonary, colonic, and mammary tumors. Cancer *89*, 2637–2645.

Thun, M.J., Namboodiri, M.M., and Heath, C.W., Jr. (1991). Aspirin use and reduced risk of fatal colon cancer. N. Engl. J. Med. *325*, 1593–1596.

Tjandrawinata, R.R., and Hughes-Fulford, M. (1997). Up-regulation of

cyclooxygenase-2 by product-prostaglandin E2. Adv. Exp. Med. Biol. *407*, 163–170.

TIsty, T.D., Romanov, S.R., Kozakiewicz, B.K., Holst, C.R., Haupt, L.M., and Crawford, Y.G. (2001). Loss of chromosomal integrity in human mammary epithelial cells subsequent to escape from senescence. J. Mammary Gland Biol. Neoplasia *6*, 235–243.

Tsujii, M., and DuBois, R.N. (1995). Alterations in cellular adhesion and apoptosis in epithelial cells overexpressing prostaglandin endoperoxide synthase 2. Cell *83*, 493–501.

Tucker, O.N., Dannenberg, A.J., Yang, E.K., Zhang, F., Teng, L., Daly, J.M., Soslow, R.A., Masferrer, J.L., Woerner, B.M., Koki, A.T., and Fahey, T.J., 3rd. (1999). Cyclooxygenase-2 expression is up-regulated in human pancreatic cancer. Cancer Res. *59*, 987–990.